Study of $B \to K$ decays

2015 J. Phys.: Conf. Ser. 631 012036

(http://iopscience.iop.org/1742-6596/631/1/012036)

Journal of Physics: Conference Series **631** (2015) 012036 doi:10.1088/1742-6596/631/1/012036

Study of $B \to K\pi\pi\gamma$ decays

Alessandro Pilloni on behalf of the *BABAR* Collaboration

"Sapienza" Università di Roma, Dipartimento di Fisica and INFN, P.le Aldo Moro 5, I-00181 Roma, Italy

E-mail: alessandro.pilloni@roma1.infn.it

Abstract. In $b \to s\gamma$ transitions, the Standard Model predicts that B^0 ($\overline{B}^0$) decays are related predominantly to the presence of right- (left-) handed photons in the final state. Therefore, the mixing-induced *CP* asymmetry in $B \to f_{CP}\gamma$ decays is expected to be small, thus being any sizeable observed asymmetries due to New Physics. In this analysis, we extract information about the $K\pi\pi$ resonant structures by means of an amplitude analysis of the $m_{K\pi\pi}$ and $m_{K\pi}$ spectra in $B^+ \to K^+\pi^-\pi^+\gamma$. The results are used, assuming isospin symmetry, to extract the mixing-induced *CP* parameters of the process $B^0 \to K^0_S\rho^0\gamma$ from the time-dependent analysis of $B^0 \to K^0_S\pi^+\pi^-\gamma$ decays without an explicit amplitude analysis of this mode.

1. Introduction

In $b \to s\gamma$ transitions, the Standard Model predicts that B^0 ($\overline{B}^0$) decays are related predominantly to the presence of right- (left-) handed photons in the final state. Therefore, the mixing-induced *CP* asymmetry in $B \to f_{CP}\gamma$ decays, where f_{CP} is a *CP* eigenstate, is expected to be small (~ 0.03 [1]). This prediction may be altered by New Physics processes, which might emit a photon with both helicity states. Moreover, decays to $K\pi\pi\gamma$ can display an interesting hadronic structure: they have contributions from several kaon resonances decaying to $K\pi\pi$. In this analysis, we extract information about the $K\pi\pi$ resonant structures by means of an amplitude analysis of the $m_{K\pi\pi}$ and $m_{K\pi}$ spectra in the charged decay channel[1] $B^+ \to K^+\pi^-\pi^+\gamma$. The results are used, assuming isospin symmetry, to extract the mixing-induced *CP* parameters of the process $B^0 \to K^0_S\rho^0\gamma$ from the time-dependent analysis of $B^0 \to K^0_S\pi^+\pi^-\gamma$ decays without an explicit amplitude analysis of this mode.

Belle has previously reported a time-dependent *CP* asymmetry measurement of $B^0 \to K^0_S\pi^+\pi^-\gamma$ decays [2]. Similar measurements with $B^0 \to K^0_S\pi^0\gamma$ decays have been reported by *BABAR* [3] and Belle [4]. At this time the measured *CP* asymmetry parameters are compatible with SM predictions, and no evidence of NP has been observed. LHCb has recently performed a study about the photon polarization in $B^+ \to K^+\pi^-\pi^-\gamma$ decay, via the distribution of the angle of the photon with respect to plane defined by the final state hadrons [5]. Studies of the processes $B^+ \to K^+\pi^+\pi^-\gamma$ and $B^0 \to K^0_S\pi^-\pi^+\gamma$ including measurements of the branching fractions have been performed by both *BABAR* [6] and Belle [7]. The latter also finds the branching fraction of the resonant decay $B^+ \to K_1(1270)^+\gamma$.

2. Analysis strategy

The present study aims to perform a time-dependent analysis of $B^0 \to K^0_S\pi^+\pi^-\gamma$ decays to extract the direct and mixing-induced *CP* asymmetry parameters, $\mathcal{C}_{K^0_S\rho\gamma}$ and $\mathcal{S}_{K^0_S\rho\gamma}$, in the $B^0 \to K^0_S\rho^0\gamma$ mode. However, due to the large natural width of the $\rho^0(770)$, a non negligible amount of $B^0 \to K^{*\pm}(K^0_S\pi^\pm)\pi^\mp\gamma$ events, which are not *CP* eigenstates and do not contribute to $\mathcal{S}_{K^0_S\rho\gamma}$, are expected to lie under the $\rho^0(770)$ resonance and dilute $\mathcal{S}_{K^0_S\rho\gamma}$. We can define a dilution factor $\mathcal{D}_{K^0_S\rho\gamma}$ such as

$$\mathcal{D}_{K^0_S\rho\gamma} = \frac{\mathcal{S}_{K^0_S\pi^+\pi^-\gamma}}{\mathcal{S}_{K^0_S\rho\gamma}}, \tag{1}$$

where $\mathcal{S}_{K^0_S\pi^+\pi^-\gamma}$ is the effective value of the mixing-induced *CP* asymmetry measured for the whole $B^0 \to K^0_S\pi^+\pi^-\gamma$. This sample is expected to produce a small number of signal events, so that a proper amplitude analysis to discriminate $B^0 \to K^{*\pm}(K^0_S\pi^\pm)\pi^\mp\gamma$ from $B^0 \to K^0_S\rho^0(\pi^\mp\pi^\pm)\gamma$ is not feasible. Hence the dilution factor needs to be obtained in some other way. We decided to perform the amplitude analysis in the charged decay channel $B^+ \to K^+\pi^-\pi^+\gamma$, which has a richer statistics, and is related to $B^0 \to K^0_S\pi^+\pi^-\gamma$ by isospin symmetry. Assuming that the resonant amplitudes are the same in both modes, the dilution factor is calculated from those of $B^+ \to K^+\pi^-\pi^+\gamma$. Moreover, the amplitude analysis of

[1] Charge conjugation is implicit throughout the document.

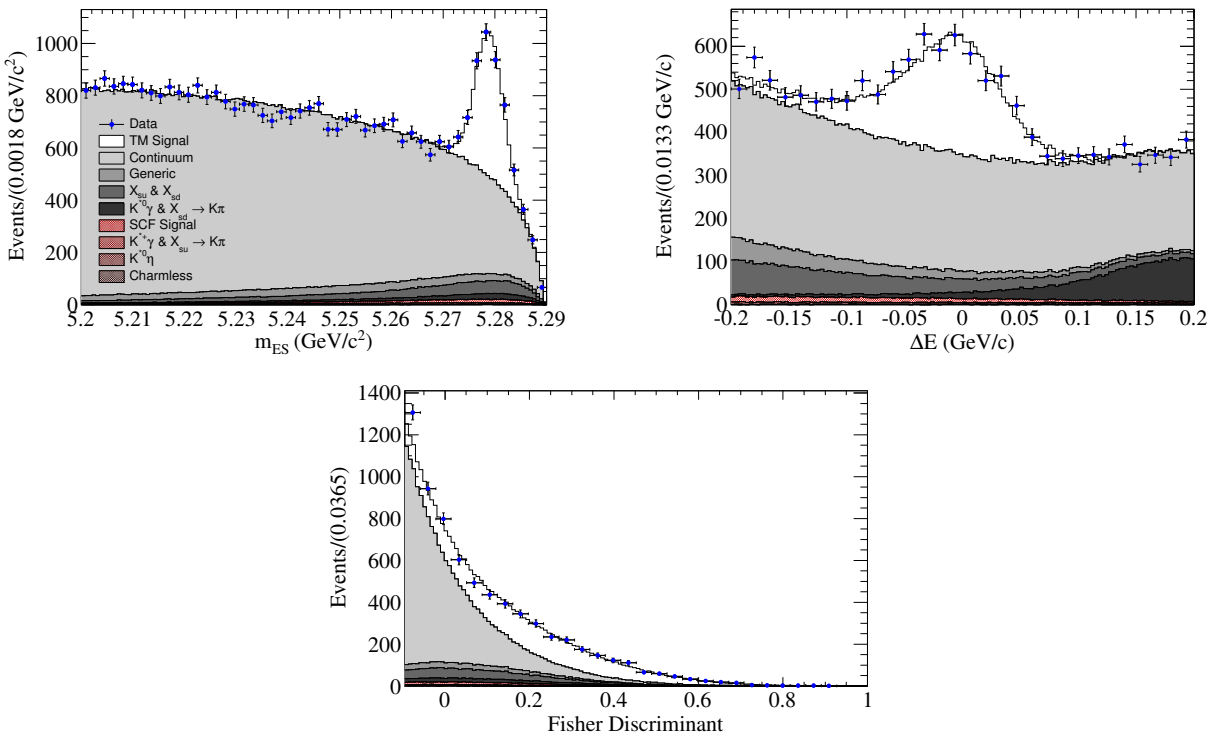

Figure 1. Distributions of $m_{\rm ES}$ (top left), ΔE (top right) and the Fisher-discriminant output (bottom) showing the fit results on the $B^+ \to K^+\pi^-\pi^+\gamma$ data sample. The distributions have their signal/background ratio enhanced by means of the following requirements: $-0.100 < \Delta E < 0.075\,\text{GeV}$ ($m_{\rm ES}$), $m_{\rm ES} > 5.27\,\text{GeV}/c^2$ (ΔE) and $m_{\rm ES} > 5.27\,\text{GeV}/c^2$; $-0.100 < \Delta E < 0.075\,\text{GeV}$ (Fisher). Points with error bars give the data. The solid histogram shows the projection of the fit result, and the shaded areas represent the contributions from different backgrounds, as described in the legend. Some of the contributions are hardly visible due to their small fractions.

$B^+ \to K^+\pi^-\pi^+\gamma$ provides also the branching fractions of $B \to K_{\rm res}\gamma$ (where $K_{\rm res}$ designates a kaonic resonance decaying to $K\pi\pi$), which are in general not well known.

We use the full dataset collected at the $\Upsilon(4S)$ resonance with the *BABAR* detector [8] at the PEP-II asymmetric-energy e^+e^- collider at the SLAC National Accelerator Laboratory. This corresponds to a total integrated luminosity of $424\,{\rm fb}^{-1}$, and to 471×10^6 $B\overline{B}$ pairs produced.

3. The charged channel $B^+ \to K^+\pi^-\pi^+\gamma$

To select the charged mode candidates, we require the center-of-mass energy of the photon to be between 1.5 and 3.5 GeV. We also require $5.200 < m_{\rm ES} < 5.292\,{\rm GeV}/c^2$ and $|\Delta E| < 200\,{\rm MeV}$. ΔE is defined as the difference between the expected and reconstructed B meson energy, $\Delta E \equiv E_B^* - \sqrt{s}/2$, where E_B^* is the reconstructed energy of the B in the e^+e^- CM frame, while $m_{\rm ES} = \sqrt{(s/2 - \mathbf{p}_B\mathbf{p}_0)^2/E_0^2 - \mathbf{p}_B^2}$, where $(E_B, \mathbf{p}_B)$ and $(E_0, \mathbf{p}_0)$ are the four-vectors of the B-candidate and of the CM frame, respectively. Charged particle identication is performed to assign the pion and kaon hypotheses. We also reject events where the γ comes from a π^0 or a η.

We first perform an unbinned extended maximum-likelihood fit to data to extract the yield of $B^+ \to K^+\pi^-\pi^+\gamma$ signal events. The fit uses the variables ΔE, $m_{\rm ES}$, and the Fisher-discriminant output to discriminate signal events from background. The Fisher-discriminant combine six discriminating variables related to the shape of the event. Using information from the maximum likelihood fit, the $m_{K\pi\pi}$, $m_{K\pi}$ and $m_{\pi\pi}$ spectra in signal events (where m_X is the invariant mass of the X particle system) are extracted using the ${}_s\mathcal{P}lot$ technique [9]. The results are shown in Figure 1. A signal yield of $2441 \pm 91^{+34}_{-57}$ is observed.

We perform a fit to the signal ${}_s\mathcal{P}lot$ of $m_{K\pi\pi}$ in order to extract from data the branching fractions of kaonic resonances decaying to $K^+\pi^-\pi^+$. We model the $m_{K\pi\pi}$ distribution as a coherent sum of five Relativistic Breit-Wigner (RBW) line shapes, with constant widths. Since helicity angles are not explicitly taken into account, the interference occurs between resonances with same J^P only. The result of the fit is shown in Figure 2, and the branching fractions obtained are given in Table 1.

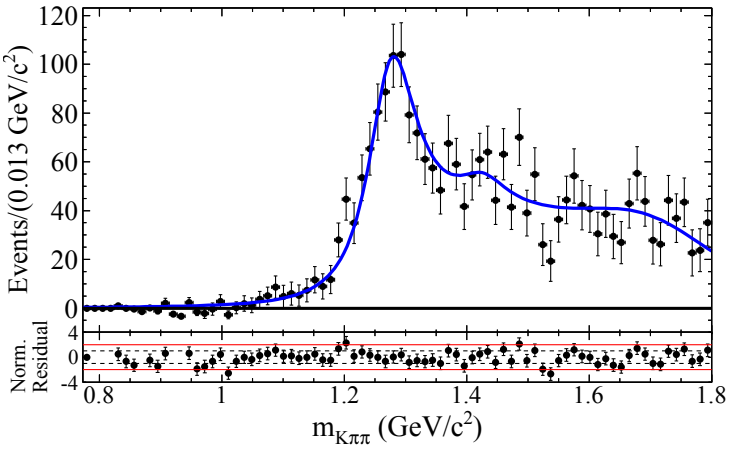

Figure 2. Distribution of $m_{K\pi\pi}$ for $B^+ \to K^+\pi^-\pi^+\gamma$ signal events (${}_s\mathcal{P}lot$), extracted from the maximum likelihood fit to $m_{\rm ES}$, ΔE and the Fisher discriminant. Points with error bars give the sum of ${}_sWeights$. The blue solid curve is the result of the fit performed directly to this $m_{K\pi\pi}$ distribution to extract the different contributions from kaonic resonances decaying to $K^+\pi^-\pi^+$. Below each bin are shown the residuals, normalized in error units. The parallel dotted and full lines mark the 1σ and 2σ levels, respectively.

Table 1. Branching fractions of the different $K_{\rm res}$ decaying into $K^+\pi^-\pi^+$, extracted from the fit to the $m_{K\pi\pi}$ spectrum. The quoted numbers are obtained using the fit fraction of each component and the corresponding efficiency. To correct for the secondary branching fractions we use the values from PDG [10]. The upper limit reported are at 90% C.L.. The first uncertainty is statistical, the second is systematic, and the third, when present, is due to the uncertainties on the secondary branching fractions.

Mode	$\mathcal{B}(B^+ \to \text{Mode}) \times \mathcal{B}(K_{\rm res} \to K^+\pi^-\pi^+) \times 10^6$	$\mathcal{B}(B^+ \to \text{Mode}) \times 10^6$	PDG values ($\times 10^6$)
Inclusive $B^+ \to K^+\pi^-\pi^+\gamma$	$\cdots$	$27.2 \pm 1.0^{+1.1}_{-1.3}$	27.6 ± 2.2
$K_1(1270)^+\gamma$	$14.5^{+2.0+1.1}_{-1.3-1.2}$	$44.0^{+6.0+3.5}_{-4.0-3.7} \pm 4.6$	43 ± 13
$K_1(1400)^+\gamma$	$4.1^{+1.9+1.3}_{-1.2-0.8}$	$9.7^{+4.6+3.1}_{-2.9-1.8} \pm 0.6$	< 15
$K^*(1410)^+\gamma$	$9.7^{+2.1+2.4}_{-1.9-0.7}$	$23.8^{+5.2+5.9}_{-4.6-1.4} \pm 2.4$	$\varnothing$
$K_2^*(1430)^+\gamma$	$1.5^{+1.2+0.9}_{-1.0-1.4}$	$10.4^{+8.7+6.3}_{-7.0-9.9} \pm 0.5$	$< 14 \pm 4$
$K^*(1680)^+\gamma$	$17.0^{+1.7+3.5}_{-1.4-3.0}$	$71.7^{+7.2+15}_{-5.7-13} \pm 5.8$	< 1900

We then extract the intermediate resonances decaying into $K^+\pi^-$ and $\pi^+\pi^-$. The limited statistics does not allow to perform a full two-dimensional amplitude analysis, so we perform a binned maximum-likelihood fit to the signal ${}_s\mathcal{P}lot$ of the projected $m_{K\pi}$ variable. The spectrum is modeled as the projection of two 1^- and one 0^+ components. The vector components are the $\rho^0(770)$ (described with a Gounaris-Sakurai lineshape), and the $K^{*0}(892)$ (described with a Relativistic Breit-Wigner). The scalar component is modeled by the LASS parametrization [11], which consists of the $K_0(1430)^0$ resonance together with an effective range non-resonant component. Both in the fit to the $m_{K\pi\pi}$ and the $m_{K\pi}$ spectra, we measure directly the magnitudes and phases of the different components of the corresponding signal model. The amplitudes of the different kaonic resonances extracted from the fit to $m_{K\pi\pi}$ are used to compute their fit fractions. These, in turn, are used to extract branching fractions of the different $K_{\rm res}$ contributions, that are used as inputs to the $m_{K\pi}$ fit model. The result of the fit is given in Figure 3, and gives the amplitudes of the three $K^+\pi^-$ and $\pi^+\pi^-$ intermediate states. In order to optimize the sensitivity on $\mathcal{S}_{K^0_S\rho\gamma}$, to calculate the dilution factor, we apply the additional cuts $600 < m_{\pi\pi} < 900\,\text{MeV}/c^2$, in order to enhance the proportion of the $\rho^0(770)$, and we apply a veto on the $K^{*0}(892)$ requiring $m_{K\pi} < 845 \wedge m_{K\pi} > 945\,\text{MeV}/c^2$. We obtain the dilution factor:

$$\mathcal{D}_{K^0_S\rho\gamma} = 0.549^{+0.096}_{-0.094}, \tag{2}$$

where the quoted uncertainties are sums in quadrature of statistical and systematic uncertainties. The branching fractions obtained are reported in Table 2.

4. The neutral channel $B^0 \to K^0_S\pi^+\pi^-\gamma$

In the neutral decay mode, the event are selected with the same criteria as in the charged mode analysis. The K^+ is replaced with a $K^0_S \to \pi^+\pi^-$ candidate, which is required to have a mass within $11\,\text{MeV}/c^2$ from the nominal value [10], and a lifetime significance $> 5\sigma$, to ensure the decay vertices of the B^0 and K^0_S to be well separated. In addition, we require the cosine of the angle between the K^0_S flight direction and the vector connecting the B-daughter pions and the K^0_S vertex to be > 0.995, to suppress combinatiorial background. The time difference Δt is obtained from the measured distance between the decay vertices positions of the fully reconstructed B^0 candidate ($B^0_{\rm rec}$) and of the other one ($B^0_{\rm tag}$). The distance is transformed to

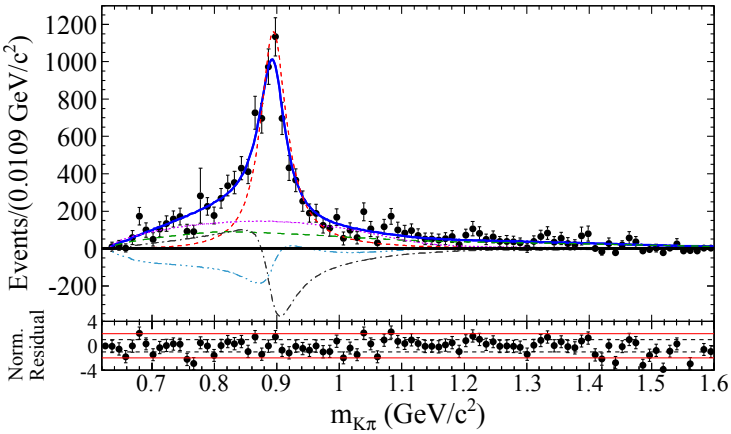

Figure 3. Distribution of $m_{K\pi}$ for $B^+ \to K^+\pi^-\pi^+\gamma$ signal events ($_s\mathcal{P}lot$), extracted from the maximum likelihood fit to $m_{\rm ES}$, ΔE, and the Fisher discriminant. Points with error bars give the sum of $_sWeights$. The blue solid curve is the result of the fit performed directly to this $m_{K\pi}$ distribution to extract the different contributions from $K\pi$ and $\pi\pi$ intermediate states. The small-dashed red, medium-dashed green and dotted magenta curves correspond to the $K^{*0}(892)$, $\rho^0(770)$ and $(K\pi)$ S-wave contributions, respectively. The dashed-dotted gray curve corresponds to the interferences between the two P-wave components, *i.e.* the $K^{*0}(892)$ and the $\rho^0(770)$, while the dashed-triple-dotted light blue curve corresponds to the interferences between the $(K\pi)$ S-wave and the $\rho^0(770)$.

Table 2. Branching fractions of the different resonances decaying to $K\pi$ and $\pi\pi$, extracted from the fit to the $K^+\pi^-$ spectrum. The quoted numbers are obtained using the fit fraction of each component and the corresponding efficiency. R denotes an intermediate resonant state and h stands for the final state K, π.. To correct for the secondary branching fractions we used the values from PDG [10] and $\mathcal{B}\left(K^{*0}(892) \to K^+\pi^-\right) = \frac{2}{3}$. The first uncertainty is statistical, the second is systematic, and the third, when applicable, is due to the uncertainties on the secondary branching fractions. The last two rows of the table are obtained by separating the contributions from the resonant and the non-resonant part of the LASS parametrization.

Mode	$\mathcal{B}(B^+ \to \text{Mode}) \times \mathcal{B}(R \to hh) \times 10^6$	$\mathcal{B}(B^+ \to \text{Mode}) \times 10^6$	PDG values ($\times 10^6$)
Inclusive $B^+ \to K^+\pi^-\pi^+\gamma$	$\cdots$	$27.2 \pm 1.0^{+1.1}_{-1.3}$	27.6 ± 2.2
$K^{*0}(892)\pi^+\gamma$	$17.3 \pm 0.9^{+1.2}_{-1.1}$	$26.0^{+1.4}_{-1.3} \pm 1.8$	20^{+7}_{-6}
$K^+\rho^0(770)\gamma$	$9.1^{+0.8}_{-0.7} \pm 1.3$	$9.2^{+0.8}_{-0.7} \pm 1.3 \pm 0.02$	< 20
$(K\pi)^{*0}_0\pi^+\gamma$	$11.3 \pm 1.5^{+2.0}_{-2.6}$	$\cdots$	$\varnothing$
$(K\pi)^0_0\pi^+\gamma$ (NR)	$\cdots$	$10.8^{+1.4+1.9}_{-1.5-2.5}$	< 9.2
$K^*_0(1430)^0\pi^+\gamma$	$0.51 \pm 0.07^{+0.09}_{-0.12}$	$0.82 \pm 0.11^{+0.15}_{-0.19} \pm 0.08$	$\varnothing$

Δt using the known boost $\beta\gamma = 0.56$ of the e^+e^- system. The candidates are rejected when $|\Delta t| > 20$ ps, or if the error on Δt is higher than 2.5 ps. To determine the flavor of $B^0_{\rm tag}$, we use the B flavor-tagging algorithm described in Ref. [12].

We perform an unbinned extended maximum-likelihood fit to data to extract the yield of $B^0 \to K^0_S\pi^+\pi^-\gamma$ signal events. We consider also the additional selection cuts on $m_{\pi\pi}$ and $m_{K\pi}$ considered when computed $\mathcal{D}_{K^0_S\rho\gamma}$. The fit uses the variables ΔE, $m_{\rm ES}$, and the Fisher-discriminant. The including of time-dependence in the fit allows the determination of mixing-

induced *CP* violation and provides additional continuum background rejection. The signal time-dependent decay rate is given by

$$\mathcal{P}\left(\Delta t, \sigma_{\Delta t}\right) = \frac{e^{-|\Delta t|/\tau_{B^0}}}{4\tau_{B^0}} \times \left[1 + q_{\rm tag}\frac{\Delta D^c}{2} - q_{\rm tag}\left\langle D\right\rangle^c \mathcal{C}\cos\left(\Delta m_d \Delta t\right) + q_{\rm tag}\left\langle D\right\rangle^c \mathcal{S}\sin\left(\Delta m_d \Delta t\right)\right] \otimes \mathcal{R}^c\left(\Delta t, \sigma_{\Delta t}\right), \quad (3)$$

where $q_{\rm tag}$ is the flavor-tag of the event: $q_{\rm tag} = -1$ for $B_{\rm rec} = B^0$, and $+1$ for $B_{\rm rec} = \overline{B}^0$, τ_{B^0} is the B^0 lifetime and Δm_d is the $B^0\overline{B}^0$ oscillation frequency, fixed to the measurement from Ref. [12]. The parameters $\langle D\rangle^c$ and ΔD^c are related to the mistag probability, and to the performance difference for the two tags, respectively. The resolution function $\mathcal{R}$, takes into account the imperfect measurement of Δt. The coefficients $\mathcal{S}$ and $\mathcal{C}$ are the parameters associated with mixing-induced *CP* violation and direct *CP* violation, respectively.

The maximum-likelihood fit to data yields $245 \pm 24^{+13}_{-16}$ signal events, which results in an inclusive branching fraction of

$$\mathcal{B}\left(B^0 \to K^0_S\pi^+\pi^-\gamma\right) = \left(23.9 \pm 2.4^{+1.6}_{-1.9}\right) \times 10^{-6}. \quad (4)$$

In both cases, the first quoted uncertainty is statistical and the second is systematic. Figure 4 shows signal-enhanced distributions of the four discriminating variables in the fit. The result of the fit to data for the time-dependent *CP* violation parameters in signal events is

$$\mathcal{S}_{K^0_S\pi^+\pi^-\gamma} = +0.14 \pm 0.25^{+0.04}_{-0.03}, \quad (5)$$

$$\mathcal{C}_{K^0_S\pi^+\pi^-\gamma} = -0.39 \pm 0.20 \pm 0.05. \quad (6)$$

We finally obtain $\mathcal{S}_{K^0_S\rho\gamma}$ dividing $\mathcal{S}_{K^0_S\pi^+\pi^-\gamma}$ by the $\mathcal{D}_{K^0_S\rho\gamma}$ given in Eq. (2):

$$\mathcal{S}_{K^0_S\rho\gamma} = 0.249 \pm 0.455^{+0.076}_{-0.060}, \quad (7)$$

which is compatible with the SM expectation of ~ 0.03 [1].

5. Systematic uncertaintiess

In the analysis of $B^+ \to K^+\pi^-\pi^+\gamma$ decays, we considered different sources of systematic uncertainties affecting the amplitudes in the $m_{K\pi\pi}$ and $m_{K\pi}$ spectra. These have been propagated to the dilution factor $\mathcal{D}_{K^0_S\rho\gamma}$ and to the branching fractions calculated from the amplitudes. As for the $K_{\rm res}$ amplitudes, we account for effects from the fixed parameters in the maximum-likelihood fit, the fixed line-shape parameters of the kaonic resonances in the fit model, the effects of adding other resonances at high masses to the fit model, the procedure of the $m_{K\pi\pi}$ ${}_s\mathcal{P}lot$ extraction, as well as the binning in the fitted distribution. The dominant systematic uncertainty originates from the fixed line-shape parameters of the resonances. The amplitudes extracted from the $m_{K\pi}$ spectrum are affected mostly by the weights of the kaonic resonances obtained in the $m_{K\pi\pi}$ fit. Specific sources of systematic uncertainties are also taken into account for the extraction of branching fractions, like the uncertainties on the number of $B\overline{B}$ pairs recorded in the full *BABAR* dataset, the input branching fractions, and other detector-related systematics. Similarly, for the neutral $B^0 \to K^0_S\pi^+\pi^-\gamma$ channel, systematics due to the fixed parameters in the maximum likelihood fit have been considered.

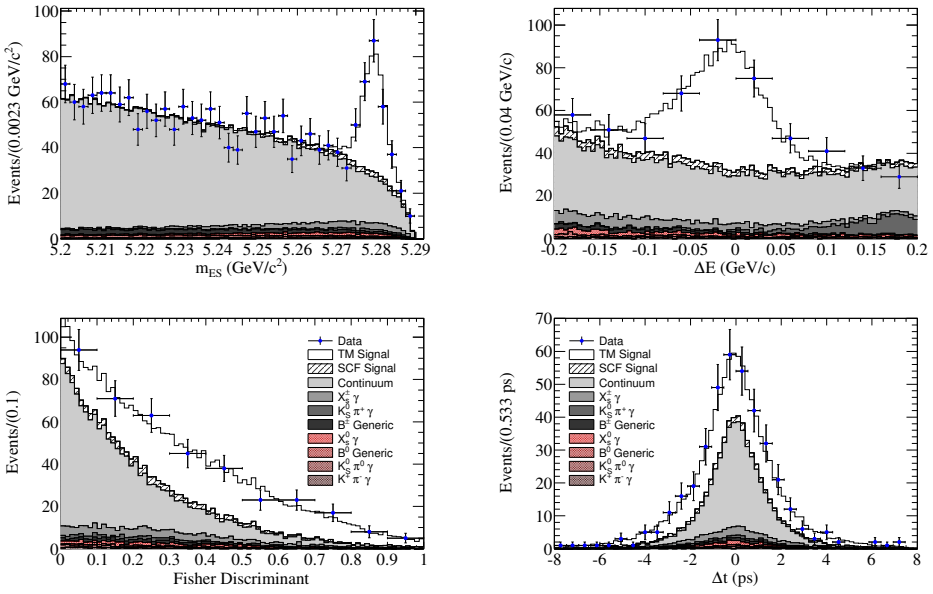

Figure 4. Distributions of $m_{\rm ES}$ (top left), ΔE (top right), the Fisher-discriminant output (bottom left), and Δt (bottom right), showing the fit results on the $B^0 \to K^0_S\pi^+\pi^-\gamma$ data sample. The distributions have their signal/background ratio enhanced by means of the following requirements: $-0.15 \leq \Delta E \leq 0.10\,\text{GeV}$ ($m_{\rm ES}$), $m_{\rm ES} > 5.27\,\text{GeV}/c^2$ (ΔE) and $m_{\rm ES} > 5.27\,\text{GeV}/c^2$; $-0.15 \leq \Delta E \leq 0.10\,\text{GeV}$ (Fisher and Δt).

6. Conclusions

The *BABAR* Collaboration, seven years after the shutdown of the experiment, is still producing competitive results. We have presented a measurement of the time-dependent *CP* asymmetry in the radiative-penguin decay $B^0 \to K^0_S\rho^0\gamma$, using the full *BABAR* dataset recorded at the $\Upsilon(4S)$ peak. We obtain the *CP*-violating parameters $\mathcal{S}_{K^0_S\pi^+\pi^-\gamma} = +0.14 \pm 0.25^{+0.04}_{-0.03}$, and $\mathcal{C}_{K^0_S\pi^+\pi^-\gamma} = -0.39 \pm 0.20 \pm 0.05$, where the first quoted errors are statistical and the second are systematic. We extract from this measurement the time-dependent *CP* asymmetry related to the hadronic *CP* eigenstate $\rho^0 K^0_S$ and obtain $\mathcal{S}_{K^0_S\rho\gamma} = 0.25 \pm 0.46^{+0.08}_{-0.06}$. This observables is related to the photon polarization of the underlying $b \to s\gamma$ transition. The dilution factor has been extracted from the higher statistics charged mode $B^+ \to K^+\pi^-\pi^+\gamma$, assuming isospin symmetry, via the study of the resonant structures. Moreover, the branching fractions of the different $K_{\rm res} \to K\pi\pi$ states and the overall branching fractions of the $\rho^0 K^+$, $K^{*0}\pi^+$, and $(K\pi)_{S\text{-wave}}\pi^+$ are also measured.

References

[1] Atwood D, Gershon T, Hazumi M and Soni A 2005 *Phys.Rev.* **D71** 076003 (*Preprint* hep-ph/0410036)
[2] Li J *et al.* (Belle Collaboration) 2008 *Phys.Rev.Lett.* **101** 251601 (*Preprint* 0806.1980)
[3] Aubert B *et al.* (*BABAR* Collaboration) 2008 *Phys.Rev.* **D78** 071102 (*Preprint* 0807.3103)
[4] Ushiroda Y *et al.* (Belle Collaboration) 2006 *Phys.Rev.* **D74** 111104 (*Preprint* hep-ex/0608017)
[5] Aaij R *et al.* (LHCb Collaboration) 2014 *Phys.Rev.Lett.* **112** 161801 (*Preprint* 1402.6852)
[6] Aubert B *et al.* (*BABAR* Collaboration) 2007 *Phys.Rev.Lett.* **98** 211804 (*Preprint* hep-ex/0507031)
[7] Yang H *et al.* (Belle Collaboration) 2005 *Phys.Rev.Lett.* **94** 111802 (*Preprint* hep-ex/0412039)
[8] Aubert B *et al.* (*BABAR* Collaboration) 2002 *Nucl.Instrum.Meth.* **A479** 1–116 (*Preprint* hep-ex/0105044)
[9] Pivk M and Le Diberder F R 2005 *Nucl.Instrum.Meth.* **A555** 356–369 (*Preprint* physics/0402083)
[10] Beringer J *et al.* (Particle Data Group) 2012 *Phys.Rev.* **D86** 010001
[11] Aston D, Awaji N, Bienz T, Bird F, D'Amore J *et al.* 1988 *Nucl.Phys.* **B296** 493
[12] Aubert B *et al.* (*BABAR* Collaboration) 2007 *Phys.Rev.Lett.* **99** 171803 (*Preprint* hep-ex/0703021)